

High Efficiency and Tribology in Rolling Bearings

H. MATSUYAMA

Rolling bearings widely used to support rotating shafts in various industrial machineries are based on tribology. Tribology is the science and technology of interacting surfaces in relative motion and of related subjects and practices and is an engineering technology that deals with friction, wear, lubrication, etc. This report explains the lubrication theory of rolling bearings with a focus on elastohydrodynamic lubrication (EHL) and gives examples of applying tribology to the high efficiency technology for tapered roller bearings that are used in a variety of automotive applications.

Key Words: tribology, friction, lubrication, rolling bearing, EHL, tapered roller bearing

1. Introduction

Tribology is a science technology that deals with friction, wear, and lubrication, covering a diverse area such as surfaces, contact, surface damage and extending to lubricants, materials and so forth. Rolling bearings are mechanical elements utilizing the rolling motion of parts called rolling elements to guide rotation while supporting load. Rolling bearings are used as support for rotating shafts in a wide range of industrial machinery, and by reducing friction, contribute to the reduction of energy consumption and heat generation, the suppression of wear, the improvement of reliability and so forth. In order to contribute to better fuel and energy efficiency in vehicles aiming to lower CO₂ emissions, there is a demand for high efficiency in rolling bearings, and as such the role of tribology is ever important. This report explains the lubrication theory of rolling bearings with a focus on elastohydrodynamic lubrication and gives examples of applying tribology to increase the efficiency of tapered roller bearings used in a variety of automotive applications, such as transmissions, differentials and so forth.

2. Lubrication Theory of Rolling Bearings

2.1 Elastohydrodynamic Lubrication

On lubricant surfaces in an outer contact state such as rolling bearings or gears, load is concentrated in an extremely narrow contact area therefore contact pressure is high and the elastic deformation of contact surfaces cannot be ignored. The hydrodynamic lubrication regime where this type of elastic deformation influence appears is called elastohydrodynamic lubrication (EHL). Dowson et al.¹⁾ clarified that by applying Reynolds' theory on hydrodynamic lubrication with consideration to the

increase due to pressure of elastic deformation of contact surfaces and lubricant viscosity, that the fluid film would be formed even when contact was concentrated. **Figure 1** shows the EHL pressure distribution and film profile at line contact. The film profile is consistent (central film thickness) almost throughout the entire contact zone however in order to respond to the sudden drop in pressure at the exit of the contact area, the film thickness becomes constricted and the minimum film thickness portion is formed. EHL pressure distribution is close to the Hertzian contact pressure distribution, however at the entrance a pressure zone due to a wedge effect is recognized and pressure peaks (pressure spikes) immediately before the film thickness is constricted near the exit.

Based on numerical analysis results, Dowson et al. derived the below equation for calculating minimum film thickness at line contact¹⁾.

$$h_{\min} = 2.65 U^{0.7} G^{0.54} W^{-0.13} \cdot R \quad (1)$$

Where, h_{\min} is the minimum film thickness and U , G , W are the speed, material and load parameters, respectively, while R is the equivalent radius. EHL film thickness is heavily affected by speed, viscosity and the pressure viscosity coefficient, therefore the effect of load is minimal.

Moreover, Dowson et al. extended the EHL theory from line contact to the more commonplace point contact^{2), 3)}. **Figure 2** is an observation of EHL film distribution at point contact using optical interferometry⁴⁾. The central film thickness h_c and minimum film thickness h_{\min} are obtained using the Chittenden-Dowson-Dunn-Taylor's equations³⁾.

$$h_c = 4.31 U^{0.68} G^{0.49} W^{-0.073} \times (1 - e^{-1.23k}) \cdot R_x \quad (2)$$

$$h_{\min} = 3.68 U^{0.68} G^{0.49} W^{-0.073} \times (1 - e^{-0.67k}) \cdot R_x \quad (3)$$

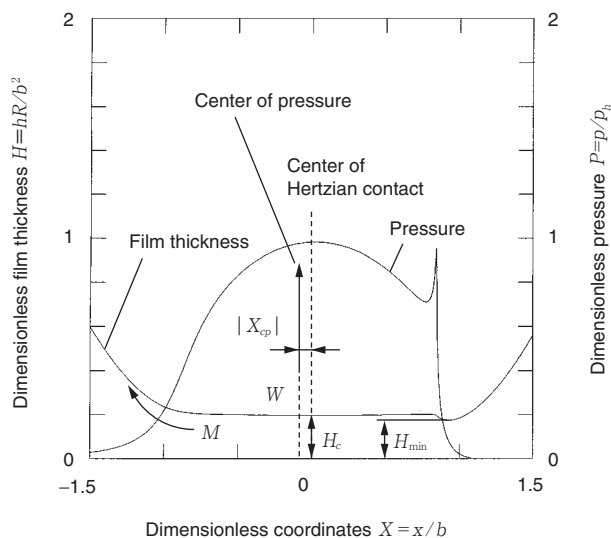


Fig. 1 EHL pressure distribution and film profile at line contact

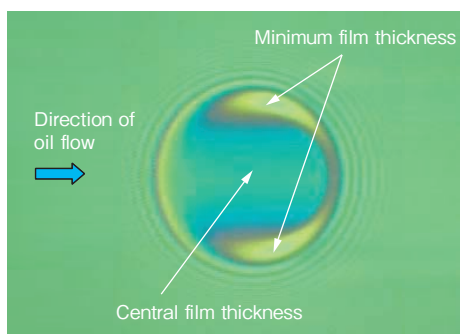


Fig. 2 Observation of EHL film thickness distribution

Where, k is the ellipticity of the contact ellipse and is applied as $k = (R_y/R_x)^{2/3}$. R_x and R_y are equivalent radii in the rolling direction and in the direction perpendicular to this rolling direction, respectively. The author and co-worker⁴⁾ confirmed in experiments that the film thickness across the wide area of k was consistent with the calculated film thickness obtained from equations (2) and (3). It is possible to predict the oil film thickness of ball bearing raceways and tapered roller bearing ribs using these same equations.

2. 2 EHL and Surface Roughness

The main aims of rolling bearing lubrication are to form lubricant film between rolling elements and the bearing raceways to prevent wear and damage such as seizure, and to reduce rolling fatigue life by avoiding direct metal contact between rolling elements and the bearing raceways. If metal contact does occur between the surface roughness protrusions (interference between protrusions), the contact stress will be extremely high, causing cracks to occur from the surface and resulting

in premature peeling. In general, film parameter Λ is used as the index to evaluate the degree of protrusion-to-protrusion interference in the EHL zone.

$$\Lambda = h_0 / \sigma = h_0 / (\sigma_1^2 + \sigma_2^2)^{1/2} \tag{4}$$

Where, h_0 is the film thickness, while σ_1 and σ_2 are the root-mean-square values of roughness. When $\Lambda > 3$, the two applicable sections are practically always separated from each other by the film, therefore the effect of surface roughness can practically be ignored. However, if Λ is less than 3, interference will occur between protrusions and when $\Lambda < 1$, the two applicable sections will almost always be in contact⁵⁾.

2. 3 EHL Viscous Rolling Resistance

Rolling friction is approximately 1/10 to 1/1 000 the size of sliding friction. However, when rolling motion occurs in an EHL state, the pressure distribution becomes asymmetrical as shown in **Fig. 1**, therefore the central of pressure is offset from the Hertzian contact central in the direction of the entrance. That is to say, pressure distribution applies moment in the opposite direction to the rotation of rolling elements. This moment is called viscous rolling resistance. In the case of roller bearings, viscous rolling resistance is much greater than pure rolling friction and accounts for the majority of friction torque. The author and co-workers⁶⁾ performed isothermal EHL analysis using the line contact model and setting $U = 10^{-13}$ to 10^{-9} , $G = 1\ 500$ to $9\ 000$ and $W = 10^{-5}$ to 10^{-3} , derived the below equation for viscous rolling resistance m . Where, E' is the equivalent Young's modulus and l is contact length.

$$m = 14.2E' l R^2 U^{0.75} G^{-0.04} W^{0.08} \tag{5}$$

2. 4 Effect of Lubricating Oil Flow

The abovementioned equations for EHL film thickness and viscous rolling resistance are based on the assumption that there is sufficient lubricating oil in the contact zone. The author and co-workers⁶⁾ clarified that the relationship between oil starvation parameters ψ and correction coefficient β would be as per **Fig. 3** by studying the correction coefficient β obtained from the film thickness and viscous rolling resistance ratio when there is oil starvation, as opposed to when there is sufficient lubrication. As ψ decreases, in other words as oil starvation progresses, the film thickness and viscous rolling resistance decreases. It should be noted that oil starvation has a greater effect on viscous rolling resistance than it does on film thickness. This means that viscous rolling resistance, or more specifically, friction torque, can be reduced while maintaining film thickness by controlling the amount of lubricating oil.

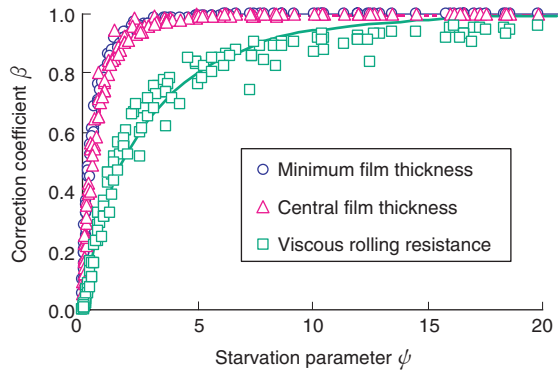


Fig. 3 Effects of oil starvation on film thickness and viscous rolling resistance

3. Application to Technologies for High Efficiency Tapered Roller Bearings

Tapered roller bearings have a large load capacity approximately 2 to 2.5 times greater than ball bearings of the same size.

Moreover, tapered roller bearings can support radial load and unidirectional axial load, are strong against impact load, and are high in stiffness. However, tapered roller bearings have a greater friction torque than ball bearings and for this reason how to reduce the torque, or to be specific, how to make high efficiency tapered roller bearings, is an issue which needs addressing.

Below, as an example of using the lubrication theory of rolling bearings to develop high efficiency tapered roller bearings^{8), 9)} deriving of equations to calculate the friction torque based on EHL theoretical analysis, the optimization of internal geometry and the reduction of lubricating oil flow are introduced as effective approaches in reducing the torque, as is the method of lubricating oil flow control that makes that possible.

3. 1 Factors Creating Friction Torque

As Fig. 4 shows, there are four factors creating the torque M in tapered roller bearings. In the low speed

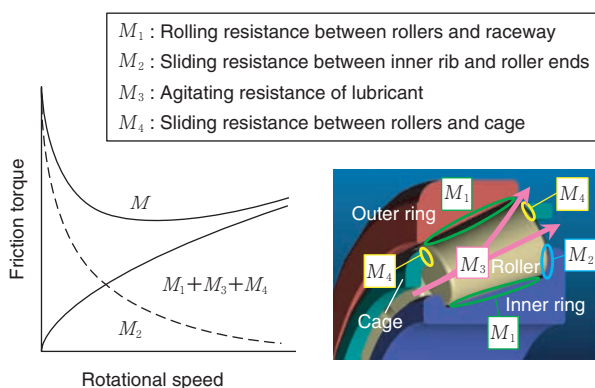


Fig. 4 Friction torque of tapered roller bearing

zone, the torque caused by M_2 is predominant due to insufficient oil film formation profile between inner rib and rollers. However, as rotational speed increases, the oil film is formed, resulting in transition to hydrodynamic lubrication, causing M_2 to decrease significantly. M_1 is created by elastic hysteresis loss and viscous rolling resistance however as the latter is predominant, the torque increases as rotational speed increases, just as in the case of M_3 . M_4 is smaller than the other factors and can be ignored.

3. 2 Optimization of Internal Geometry Based on Equations for Torque Calculation

Next, a tapered roller bearing on which only axial load is applied is considered. By solving the balancing equations for the forces and moments applied to the rollers, the torque of the tapered roller bearing can be expressed by the following equation⁷⁾.

$$M = \frac{Z}{DW} (r_o m_i + r_i m_o) + \mu \cdot e \cdot F_a \cdot \cos \gamma \quad (6)$$

Where, m_i and m_o are the viscous rolling resistances between the rollers and raceways and are obtained using equation (5). μ is the friction coefficient between the rib and the roller ends and Fig. 5⁷⁾ shows the relationship between μ and film parameter Λ . Equation (6) can be modified as per the following:

$$M = c_1 \cdot B \cdot \phi_T \cdot (N \cdot \eta_0)^{c_2} \cdot \alpha_0^{c_3} \cdot F_a^{c_4} + \mu \cdot e \cdot F_a \cdot \cos \gamma \quad (7)$$

It is presumed that the first term on the right-hand side of equation (7) expresses M_1 and M_3 while the second term expresses M_2 . As Fig. 5 shows, μ becomes practically settled at $\Lambda \geq 2$. Where, the authors measured bearing torque under the condition of $\Lambda \geq 2$, and considered the value obtained when an amount equivalent to M_2 is subtracted from the measured value to be M_1 and M_3 , correcting the coefficient and exponent of equation (7). The torque was measured in a state with sufficient oil (hereinafter, full oil flow state)⁸⁾, assuming the actual usage of differentials.

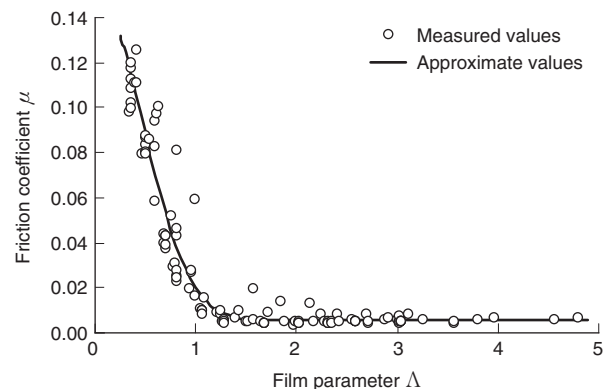


Fig. 5 Relationship between friction coefficient and film parameters

The following equations for calculating the torque of tapered roller bearings in a full oil flow state were derived based on EHL theoretical analysis and experimental analysis.

$$M = k_1 \cdot B \cdot \phi_T \cdot (N \cdot \eta_0)^{0.61} \cdot \alpha_0^{-0.04} \cdot F_a^{0.22} + \mu \cdot e \cdot F_a \cdot \cos \gamma \tag{8}$$

$$B = z^{k_2} \cdot dm^{k_3} \cdot DW^{k_4} \cdot LWR^{k_5} \cdot f(\alpha) \cdot (1 - \gamma_m^2)^{k_6} \cdot [\phi_{ci}(1 - \gamma_m)^{k_7} + \phi_{co}(1 - \gamma_m)^{k_8}] \tag{9}$$

Where, B is the coefficient determined by bearing internal geometry, ϕ_T is the thermal reduction factor, N is the inner ring rotational speed, η_0 is the viscosity of the oil under atmospheric pressure, α_0 is the pressure viscosity coefficient, F_a is axial load, e is rib-to-roller height, γ is the roller half angle, z is the number of rollers, dm is the roller pitch circle diameter, DW is the mean roller diameter, LWR is the roller effective length, γ_m is $DW \cdot \cos \theta / dm$, α is the outer raceway angle, $f(\alpha)$ is the coefficient for effect of the contact angle, ϕ_{ci} is the inner raceway crowning correction coefficient, ϕ_{co} is the outer raceway crowning correction coefficient and k_1 to k_8 are constants.

Figure 6⁸⁾ shows the effect of internal geometry on the torque. The effect on the torque of roller effective length (LWR), number of rollers (z), contact angle (α), roller pitch circle diameter (dm) and raceway crowning radii (RCo and RCi) as predicted using equations (8) and (9) are quite consistent with experimental results. **Figure 7** shows the effect of internal geometry on efficiency and load capacity based on the equations, and **Table 1** is a summary of optimum design guidelines. To create a low torque design which takes balanced performance into consideration, it is effective to make α large, z and LWR small, as well as make mean roller diameter (DW) large to suppress the reduction in load capacity which accompanies a decrease in z .

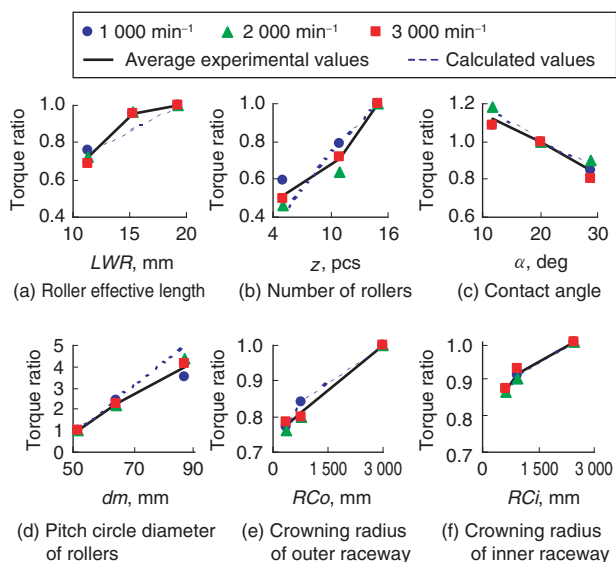


Fig. 6 Effects of internal geometry on friction torque

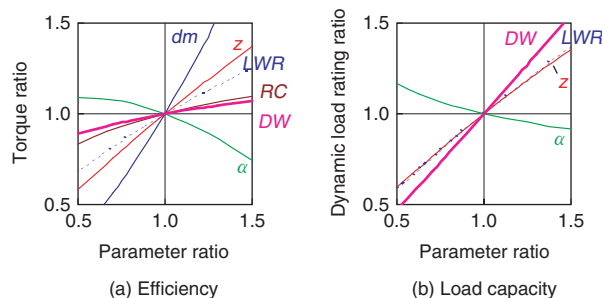


Fig. 7 Effects of internal geometry on efficiency and load capacity

Table 1 Optimum design guidelines

Bearing performance	LWR	z	α	dm	RCo	RCi	DW
High efficiency	↘	↘	↗	↘	↘	↘	↘
High capacity	↗	↗	↘	–	–	–	↗
High stiffness	↗	↗	↗	–	–	–	–
Optimum design	↘	↘	↗	↘	↘	↘	↗

↗: Increase ↘: Decrease

3. 3 Reducing Torque with Oil Flow Control

In tapered roller bearings a "pumping action" phenomenon occurs in which lubricating oil is retracted and the oil penetrates from the front to the rear of the inner ring. The oil which has infiltrated inside the bearing demonstrates complex behavior due to the revolution of the inner/outer ring and the cage, and the orbit and rotation of the rollers. This complex behavior has an effect on the occurrence of agitating resistance. The authors mounted steel fixtures on a tapered roller bearing and controlled the inflow and outflow of oil to the bearing in order to investigate the effect on the torque. The results, as shown in **Fig. 8**, showed that controlling the oil flow between the cage and small rib of the inner ring and suppressing oil stagnation inside the bearing by quick discharge, are effective measures to reducing the torque which causes agitating resistance⁸⁾.

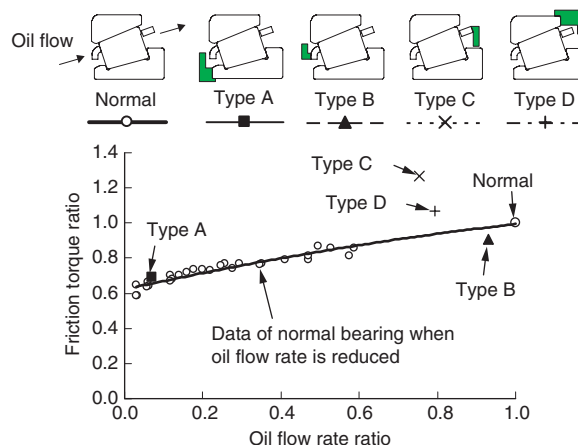


Fig. 8 Relationship between oil flow rate and friction torque

From this, as shown in Fig. 9 (a), the inner diameter of the cage was made smaller than the conventional bearings and the small rib of the inner ring was given a special shape to form a labyrinth between the cage and small rib of the inner ring, developing a structure with reduced lubricating oil flow in the bearing. Figure 10 gives detailed dimensions of the labyrinth of the developed bearing, while Fig. 11 shows the effect of each dimension in Fig. 10 on the torque and the oil flow rate. The vertical axis of Fig. 11 shows the torque ratio and the oil flow rate when axial load is 4 kN, rotational speed is 3 000 min⁻¹, oil temperature is 50°C and in a full oil flow state if the torque and the oil flow rate of a conventional bearing (Fig. 9 (b)) are set as 1. Each dimension shown on the horizontal axis of Fig. 11 is made dimensionless by inner ring bore diameter (D) and inner ring width (B). As the figure shows, the clearance in the radial direction of the cage and inner ring (X1) significantly effects the torque and the oil flow and by making X1/D smaller, the oil flow rate was reduced 60% compared with conventional bearings, while the torque was reduced by 30%. The effect of other dimensions on the torque and oil flow is minimal.

Next, as shown in Fig. 12, the torque, oil flow rate and bearing temperature rise was compared for a conventional bearing, a conventional bearing with a fixture mounted to give it a labyrinth structure (hereinafter, modified conventional bearing), and a developed bearing with a labyrinth structure and the optimum internal geometry mentioned in Section 3. 2. The experimental conditions are the same as those of Fig. 11. Experimental results are shown in Fig. 13. The modified conventional bearing has 40% less torque than the conventional bearing. However, the bearing temperature rise (difference between the bearing outer ring temperature and supplied oil temperature) is 20°C, much higher than that of the conventional bearing. This is due to less oil cooling action as a result of the oil flow rate being approximately 80% less than that of the conventional bearing. Meanwhile, the outer raceway angle has been made larger on the developed bearing, thereby increasing pumping action, meaning that the oil flow rate is higher compared with the modified conventional bearing, while the temperature rise is virtually the same as the conventional bearing. As such, there is no

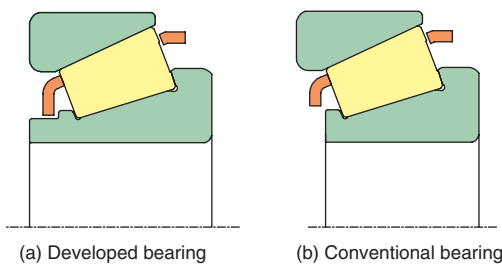


Fig. 9 Comparison between developed and conventional bearings

risk of seizure. Furthermore, the torque has been reduced by 60% compared with the conventional bearing. These results prove that the best way of reducing the torque is to combine a labyrinth structure which aims to control lubricating oil flow and an internal geometry based on the optimal design guidelines illustrated in Table 1.

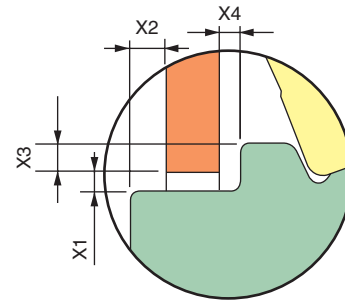
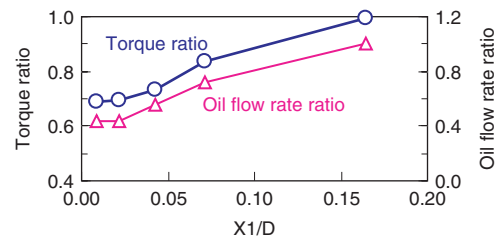
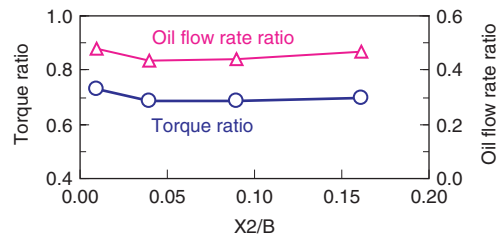


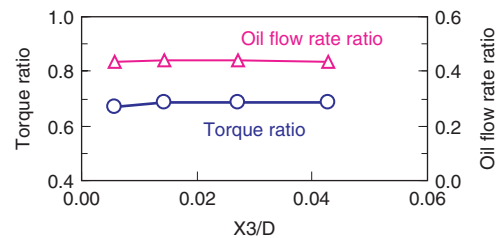
Fig. 10 Detailed dimensions of the labyrinth



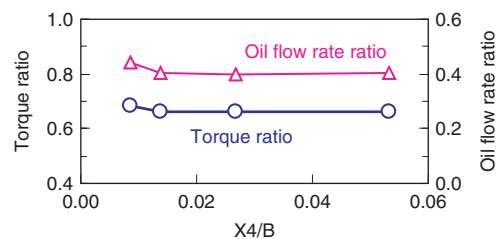
(a) Clearance in radial direction between cage and inner ring (X1)



(b) Protrusion amount of inner ring end with cage in axial direction (X2)



(c) Overlap of cage with small rib of inner ring in radial direction (X3)



(d) Clearance in axial direction between cage and inner ring (X4)

Fig. 11 Effect of each dimension on friction torque and oil flow rate

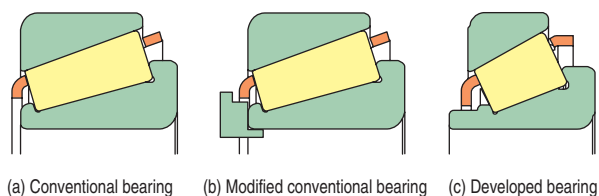


Fig. 12 Test bearings

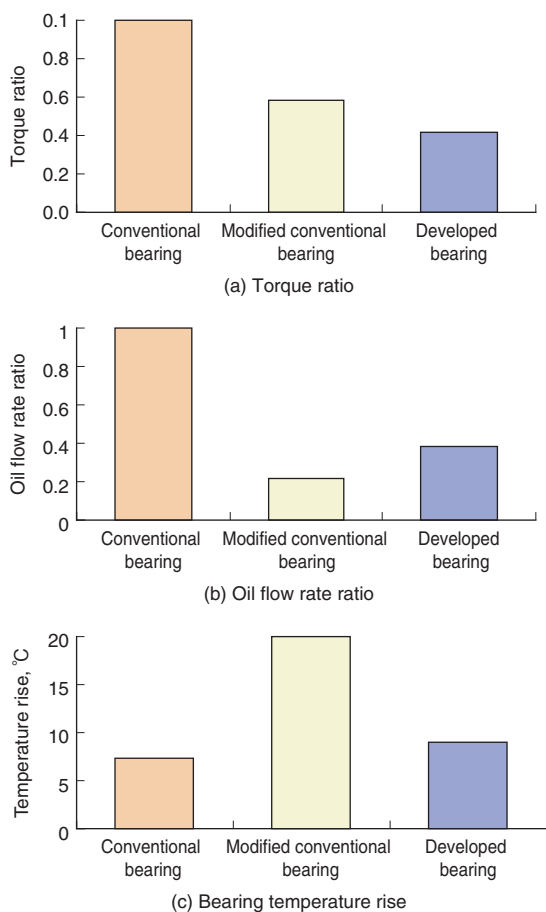


Fig. 13 Comparison of performance between developed and conventional bearings

4. Conclusion

This report has discussed the lubrication theory of rolling bearings with a focus on EHL film thickness and viscous rolling resistance. Also, as an example of application for the higher efficiency of tapered roller bearings, the deriving of equations to calculate the friction torque based on EHL theoretical analysis, the optimization of internal geometry and the reduction of lubricating oil flow were introduced as effective approaches in reducing the torque, as was the method of lubricating oil flow control that makes that possible. Each of these is an elemental technology required to create super-low friction torque tapered roller bearings^{8), 9)}, however, the same concept can be applied to ball bearings.

The term "tribology" was first conceived in Britain, which was in the midst of an economic struggle at the

time. Tribology is known to be closely linked with the economy, and it is reported that technologies based on tribology contribute to Japan's economy by around 3% of GDP. Amidst predictions that the need to reduce friction and importance of maintenance will continue to grow, tribology and rolling bearings will play an increasingly important role in not only conserving the global environment, but also in furthering the economic development of Japan and the world.

References

- 1) D. Dowson and G. R. Higginson: *Elastohydrodynamic Lubrication*, Pergamon Press (1977).
- 2) B. J. Hamrock and D. Dowson: *Ball Bearing Lubrication*, John Wiley & Sons (1981).
- 3) R. J. Chittenden, D. Dowson, J. F. Dunn and C. M. Taylor: *Proc. Roy. Soc. London*, A397 (1985) 271.
- 4) H. Matsuyama and K. Asano: *Effects of Ellipticity on EHL Oil Film Thickness*, *Proceedings of JAST Tribology Conference, Osaka* (1997) 495 (in Japanese).
- 5) Y. Yamamoto and M. Kaneta: *Tribology*, Rikougakusha (1998) 167.
- 6) H. Matsuyama, S. Kamamoto and K. Asano: *A Line Contact EHL Analysis Considering Oil Starvation*, *Proceedings of JAST Tribology Conference, Nagoya* (1998) 182 (in Japanese).
- 7) H. Matsuyama and S. Kamamoto: *Analysis of Frictional Torque in Raceway Contacts of Tapered Roller Bearings*, *Koyo Engineering Journal*, No. 159E (2001) 53.
- 8) H. Matsuyama, H. Dodoro, K. Ogino, H. Ohshima, K. Toda: *Development of Super-Low Friction Torque Tapered Roller Bearing for Improved Fuel Efficiency*, *SAE Technical Paper*, No. 2004-01-2674 (2004).
- 9) H. Matsuyama, K. Kawaguchi, A. Uemura and N. Masuda: *Super-low Friction Torque Technology of Tapered Roller Bearings for Reduction of Environmental Burdens*, *JTEKT ENGINEERING JOURNAL*, No. 1007E (2010) 47.



H. MATSUYAMA*

* *Material Engineering R&D Dept., Research & Development Center, Research & Development Headquarters*